Neoclassical Transportation in the ELMO Bumpy Torus

E. F. Jaeger, D. A. Spong, and C. L. Hedrick
Oak Ridge National Laboratory, Oak Ridge, Tennessee 37830
(Received 23 December 1977)

In the ELMO bumpy torus, neoclassical transport coefficients depend critically on the ambipolar electric field. These coefficients, calculated for arbitrary radial electric fields, are applied in a one-dimensional radial-transport calculation which, for the first time, treats the electric field self-consistently. This purely classical model predicts many features of experimental operation including a steady-state solutions with radially inward-pointing ambipolar fields.

There have been many investigations[1,2] of radial transport in axially symmetric toroidal magnetic traps such as tokamaks where lowest-order neoclassical transport is independent of radial electric fields. For axially asymmetric systems such as the bumpy torus, neoclassical transport depends sensitively on the ambipolar field, and radially resolved calculations including self-consistent ambipolar electric fields have not previously been attempted. Here we calculate neoclassical transport coefficients for the ELMO bumpy torus[3] (EBT) for arbitrary radial electric fields, and we apply these coefficients in a one-dimensional radial-transport model which includes the ambipolar field self-consistently. Previous neoclassical calculations for bumpy tori have treated only the large-electric-field limit[4] and transport in zero dimensions.[5] Self-consistent, one-dimensional calculations are necessary to predict transport scaling and stability limitations for large fusion-grade systems.

To model EBT realistically, we calculate transport coefficients without using Kovrizhnykh's[4] simplifying assumption that poloidal drifts due to electric fields dominate those due to magnetic field gradients. We use the drift kinetic equation[6] in bounce-averaged form,

$$\frac{\partial\langle f\rangle}{\partial t}+\langle\vec{v}_d\rangle\cdot\nabla\langle f\rangle+\frac{e}{mv_\parallel}\langle\vec{v}_d\rangle\cdot\vec{E}\,\frac{\partial\langle f\rangle}{\partial v_\parallel}=\langle C_f\rangle\,, \quad (1)$$

where $\langle\,\rangle$ denotes a bounce average, f is the distribution of guiding centers, $\vec{v}_d$ is the guiding center velocity, C_f is the collision operator, m is the mass, e is the charge, $\vec{E}$ is the electric field, and $v_\perp$ and $v_\parallel$ are velocity components perpendicular and parallel to the magnetic field $\vec{B}$, respectively. Assuming a purely radial electric field with no poloidal component, we separate f into an equilibrium Maxwellian part and a first-order perturbation f_1 which is Fourier analyzed in the poloidal angle θ as $f_1=\mathrm{Re}(\hat{f}_1e^{i\theta})$. A variety of collision operators has been used in Eq. (1) including the complete Fokker-Planck operator[7] and the simpler Krook models.[8] Here, we use the particle- and energy-conserving Krook model. In this case moments of Eq. (1) reduce to algebraic equations for integrals required in computing the neoclassical fluxes. This simple solution provides good agreement with results of Spong *et al.*[9] where the detailed kinetic theory is displayed for the complete Fokker-Planck operator. Our treatment of particle orbits and the θ dependence of f_1 implicitly assumes sufficiently collisional behavior that banana-shaped orbits (occurring in regions where $\vec{E}\times\vec{B}$ and grad$B$ drifts cancel) do not dominate diffusion. Such an approximation is appropriate to the collisionality of the present experiment[3] [$\nu/\Omega\sim O(1)$ where ν is the collision frequency and Ω is the poloidal drift frequency]. Particle and energy fluxes for the jth particle species may be written

$$\Gamma_{j,r}=-D_{nj}\frac{\partial n_j}{\partial r}-D_{Tj}\frac{\partial T_j}{\partial r}+n_j\mu_{nj}E_r\,,$$
$$Q_{j,r}=-K_{nj}\frac{\partial n_j}{\partial r}-K_{Tj}\frac{\partial T_j}{\partial r}+n_j\mu_{Ej}E_r\,, \quad (2)$$

where r is the radial coordinate and n and T denote density and temperature, respectively. Transport coefficients, D_{nj}, D_{Tj}, K_{nj}, and K_{Tj}, depend on three parameters, ν_j/Ω_j, $e_j\varphi/kT_j$, and $v_{0j}=2kT_j/e_jBR_T$, where R_T is the major toroidal radius, and φ is the ambipolar potential. Mobilities, μ_{nj} and μ_{Ej}, are related to D_{nj} and K_{nj} by $\mu_{nj}=(e_j/kT_j)D_{nj}$ and $\mu_{Ej}=(e_j/kT_j)K_{nj}$.

In Fig. 1, one of the transport coefficients, $D_{nj}'=D_{nj}/(v_{0j}^2/2\Omega_j)$, is explicitly displayed as a function of collisionality ν_j/Ω_j and electric potential $e_j\varphi/kT_j$ for EBT-I parameters.[3] Comparison with results of Ref. 4 shows agreement in the large-field limit ($|e_j\varphi/kT_j|\sim 100$) and enhanced diffusion at low collisionalities and finite fields. An overall geometrical scaling with the

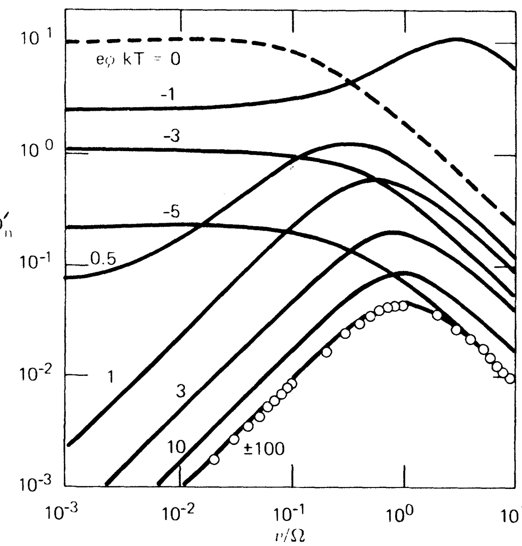

FIG. 1. Normalized density diffusion coefficient compared with the result of Ref. 4 (denoted by circles).

inverse square of the major radius R_T is evident in the dimensional factor $(v_{0j}^2/2\Omega_j)$.

In Fig. 2, Eq. (2) is used to plot electron and ion particle fluxes versus ambipolar potential. *Ad hoc* parabolic profiles are assumed for n, T, and φ characteristic of the quiescent toroidal mode in the current experiment.[3] The poloidal drift frequency Ω is obtained from two-dimensional magnetic equilibrium calculations and from analytic fits to $\Omega = 1/(eBr\tau)\partial J/\partial r$ where $J = \oint dl m v_\parallel$ and $\tau = \oint dl/v_\parallel$.[10] In the figure, quasi charge neutrality is achieved at potentials for which $\Gamma_{er} \simeq \Gamma_{ir}$. Negative potentials or radially inward-pointing electric fields are possible in the low-β plasma-core region where normal magnetic field gradients exist [Fig. 1 and Fig. 2(a)], and positive potentials or outward-pointing electric fields are predicted in the high-β electron-ring region where magnetic gradients are reversed [Fig. 2(b)].

In the absence of an electric field, ions and electrons of equal energy and pitch angle have coincident orbits and hence equal step sizes for diffusion. In this case, electrons, due to their greater collisionality, are lost $(m_i/m_e)^{1/2}$ times faster than ions. In the presence of an electric field, this flux discrepancy is equalized in one of two ways. First, a radially outward-pointing electric field can electrostatically confine electrons, reducing their flux to that of the ions as in the large-positive-field solutions in Fig. 2(a) and 2(b). Alternatively, in normal magnetic gra-

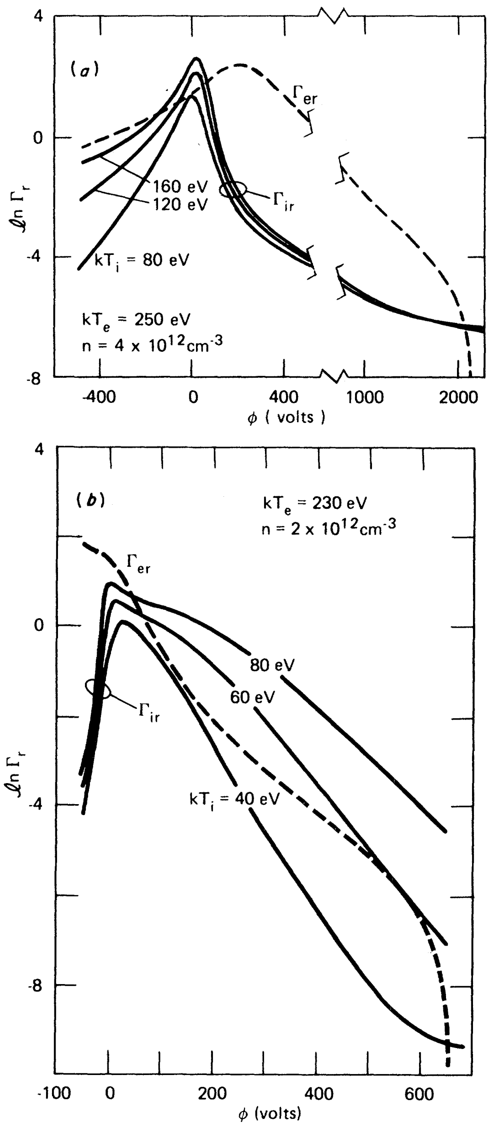

FIG. 2. Electron and ion particle flux vs ambipolar potential for (a) normal and (b) reversed magnetic field gradients.

dient regions, radially inward-pointing electric fields enhance ion diffusion by cancellation of $\vec{E} \times \vec{B}$ and grad$B$ poloidal drifts as in the negative roots in Fig. 2(a). In reversed gradient regions, outward-pointing fields enhance ion diffusion as in Fig. 2(b). Which of these scenarios is stable and consistent with power balance depends on details of radial transport, considered next.

If one neglects variation in magnetic field due to finite plasma β, as well as effects of energetic electron rings, transport due to drift waves, magnetohydrodynamic activity, and magnetic field errors, a series of moments of Eq. (1) can be derived in terms of transport coefficients defined by Eq. (2). Including the radial component of Ampere's law averaged over poloidal angle, we have

$$\begin{aligned}
&\frac{\partial n}{\partial t}=n_0\langle\sigma v\rangle_i n-\frac{1}{r}\frac{\partial}{\partial r}(r\Gamma_r),\\
&\frac{\partial}{\partial t}(\tfrac{3}{2}nkT_i)=Q_{ei}-\frac{1}{r}\frac{\partial}{\partial r}(rQ_{ir})-n_0\langle\sigma v\rangle_{\rm cx}\tfrac{3}{2}nk(T_i-T_0)+e\Gamma_{ir}E_r+n_0\langle\sigma v\rangle_i\tfrac{3}{2}nkT_0,\\
&\frac{\partial}{\partial t}(\tfrac{3}{2}nkT_e)=2m_e n\langle D_\mu\rangle-\frac{1}{r}\frac{\partial}{\partial r}(rQ_{er})-Q_{ei}-n_0\langle\sigma v\rangle_i nE_I-e\Gamma_{er}E_r,\\
&\frac{\epsilon_\perp}{e}\frac{\partial E_r}{\partial t}=\Gamma_{er}-\Gamma_{ir}=(D_{ni}-D_{ne})\frac{\partial n}{\partial r}+D_{Ti}\frac{\partial T_i}{\partial r}-D_{Te}\frac{\partial T_e}{\partial r}-n(\mu_{ni}-\mu_{ne})E_r,
\end{aligned}\qquad(3)$$

where $n\equiv n_e\simeq n_i$, $\Gamma_r\equiv\Gamma_{er}\approx\Gamma_{Ir}$, k is Boltzmann's constant, t is time, E_I is the ionization energy of atomic hydrogen, $\epsilon_\perp$ is the perpendicular plasma dielectric, and Q_{ei} is the energy exchange rate between electrons and ions. Ionization and charge-exchange rates are $n_0\langle\sigma v\rangle_i$ and $n_0\langle\sigma v\rangle_{\rm cx}$, respectively. Resonant electrons absorb microwave power at the rate[11] $2m_e n\langle D_\mu\rangle$. We assume that neutral density n_0 and temperature T_0 adjust instantly to changes in plasma parameters, allowing conventional solution of a stationary kinetic equation for the neutral velocity distribution.[12]

The equations in (3) are solved numerically with parameters corresponding to EBT-I.[3] Boundary conditions are enforced at the plasma edge ($r=a$) consistent with a cold surface plasma[3] and with a uniform isotropic source of cold neutrals at energy $E_0=0.5$ eV. The time scale for the electric field in Eq. (3) is much faster than that for the plasma parameters. Therefore, after each step on the diffusion time scale, the electric field is advanced for a sufficient time to ensure quasi charge neutrality.

Results in Fig. 3 show steady-state radial profiles of n, φ, T_e, T_i. The radially inward-pointing electric field, $E\lesssim(kT_i/e)\partial\ln B/\partial r$, corresponds to the most negative root in Fig. 2(a) and is in qualitative agreement with heavy-ion-beam measurements.[13,14] [The middle root in Fig. 2(a) is unstable by Ampere's law in Eq. (3).] Results in Fig. 3 are characteristic of toroidal-mode operation,[3] however, quantitative comparison with experiment should be regarded as tentative because of simplifying assumptions in the model.

Lowering the plasma density reduces energy transfer from electrons to ions. Ion temperature decrease until negative–electric-field solutions vanish, as in Fig. 2(a), and the system passes abruptly to the positive-field solution $E\sim-(kT_e/e)\partial\ln(nT_e^2)/\partial r$ which we find to be thermally unstable. Here, electrons are confined electrostatically, and ambipolar diffusion is dominated by ion transport which is relatively collisionless. The electric field is proportional to density and temperature gradients so that transport rates are approximately proportional to the inverse square of gradients in n and T. This produces a net positive feedback allowing gradients in n, T, and φ to become arbitrarily large near the plasma edge; no steady state is found. These solutions are thermally stable in simple point models[5] which do not include time-varying spatial scale lengths necessary for positive feedback. For negative electric fields as in Fig. 3, ambipolar diffusion is dominated by electron transport which is relatively collisional, and the electric field is less dependent on density and temperature gradients. Thus, elements necessary for positive feedback are missing and solutions are stable.

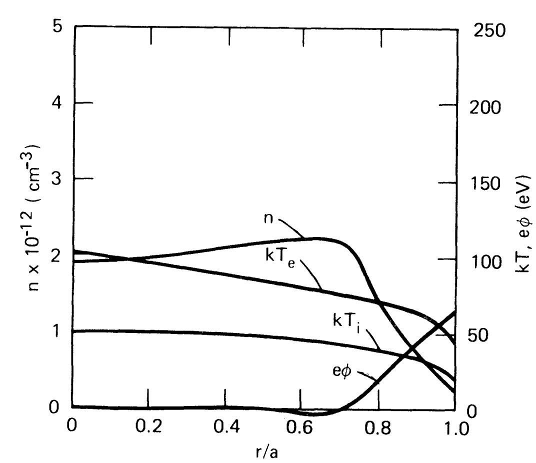

FIG. 3. Steady-state radial profiles of plasma density n, ambipolar potential φ, electron temperature kT_e, and ion temperature kT_i.

We gratefully acknowledge L. W. Owen and R. C. Goldfinger for magnetohydrodynamic equilibrium calculations, G. E. Guest and D. B. Batchelor for many helpful discussions, and R. A. Dandl and the EBT experimental group for continued confidence and support. We also thank N. A. Krall and J. B. McBride for their interest in comparing these results with those of point models. This research was sponsored by the U. S. Department of Energy under contract with Union Carbide Corporation.

[1]F. L. Hinton *et al.*, Phys. Rev. Lett. 29, 698 (1972); F. L. Hinton and R. D. Hazeltine, Rev. Mod. Phys. 48, 239 (1976).

[2]J. T. Hogan, Meth. Comput. Phys. 16, 131 (1976).

[3]R. A. Dandl *et al.*, in *Proceedings of the Fifth International Conference on Plasma Physics and Controlled Nuclear Fusion Research, Tokyo, Japan, 1974* (International Atomic Energy Agency, Vienna, Austria, 1975), Vol. II, p. 141.

[4]L. M. Kovriznykh, Zh. Eksp. Teor. Fiz. 56, 877 (1969) [Sov. Phys. JETP 29, 475 (1969)].

[5]C. L. Hedrick *et al.*, Nucl. Fusion 17, 1237 (1977); J. B. McBride and A. L. Sulton, to be published.

[6]R. D. Hazeltine, Plasma Phys. 15, 77 (1973).

[7]L. D. Landau, Zh. Eksp. Teor. Fiz. 7, 103 (1937).

[8]P. L. Bhatnager, E. P. Gross, and M. Krook, Phys. Rev. 94, 511 (1954).

[9]D. A. Spong *et al.*, Oak Ridge National Laboratory Report No. ORNL/TM-6215, 1978 (to be published).

[10]T. G. Northrop and E. Teller, Phys. Rev. 117, 215 (1960).

[11]O. Eldridge, Phys. Fluids 15, 676 (1972).

[12]J. T. Hogan and J. F. Clarke, J. Nucl. Mater. 53, (1974).

[13]P. L. Colestock *et al.*, private communication.

[14]B. H. Quon *et al.*, Oak Ridge National Laboratory Report No. ORNL-TM-6075, 1977 (to be published).

Saturation of Parametric Instabilities by Nonlinear Four-Wave Coupling

S. Y. Yuen
Francis Bitter National Magnet Laboratory, Massachusetts Institute of Technology, Cambridge, Massachusetts 02139
(Received 6 July 1977)

Nonlinear coupling of four Langmuir waves is studied as a new saturation mechanism for parametric instabilities in underdense plasmas with approximately equal electron and ion temperatures. When treated in conjunction with the usual ion nonlinear Landau damping, these processes produce a saturated Langmuir-wave spectrum with a single peak and a saturated wave energy linearly proportional to the pump intensity. These results are in good agreement with laboratory experiments.

The nonlinear saturation of parametric instabilities is directly relevant to the feasibility of applying parametric instabilities for heating plasmas.[1] In the absence of particle trapping, the dominant saturating mechanism is considered to be the multiple-decay processes, i.e., ion nonlinear Landau damping[2] if $T_e \simeq T_i$, which goes over to cascade mode coupling[3,4] when $T_e \gg T_i$ (T_e, T_i are electron and ion temperatures). These multiple-decay processes predict a saturated Langmuir-wave energy P_l proportional to the square of pump intensity, P_0^2, and a spectrum consisting of a series of peaks separated from each other by the ion acoustic frequency.

In early experiments,[5] the $P_l \propto P_0^2$ dependence can be directly inferred from absorption measurements near threshold. However, in more recent experiments[6-8] the $P_l \propto P_0^2$ relation is not observed. Mizuno and DeGroot report that for $T_e/T_i \approx 8$, $P_l \propto P_0$ from $P_0/P_{\rm th} \gtrsim 1$ to $P_0/P_{\rm th} \approx 30$.[6] Flick's experimental data at $T_e \approx T_i$ show that near threshold $P_{\rm th}$, P_l varies much faster than P_0^2, and for $P_0/P_{\rm th} \gtrsim 3$, P_l varies linearly as P_0.[7,8]

For $T_e \gg T_i$, experimentally observed steady-state Langmuir-wave spectra consist of discrete lines[9] in agreement with cascade mode-coupling theories.[3,4] When $T_e \approx T_i$, nonlinear ion Landau damping theories[2] predict a similar spectrum. However, although the theoretically predicted spectrum is consistent with ionosphere measurements,[10] it is not consistent with laboratory experiments.[7,8] Instead, Flick reports an essentially single-peaked spectrum for $P_0/P_{\rm th}$ varying from 1 to 10. Since distinct peaks are fine structures and may not be experimentally resolved, it is important to note that while previous theories predict wave energy being spread into modes with much lower wave vector via secondary ion non-